

Multiobjective Optimal Design of Wireless Power Transfer Devices using a Genetic Algorithm and Accurate Analytical Formulae

A. Desmoort, *Student Member, IEEE*, Z. De Grève, *Member, IEEE*, and O. Deblecker, *Member, IEEE*
University of Mons, Electrical Power Engineering Unit, Bd Dolez 31, 7000 Mons, Belgium
{alexis.desmoort,zacharie.degrev,olivier.deblecker}@umons.ac.be

Abstract—In this work, the Non-dominated Sorting Genetic Algorithm (NSGA) is employed for the multiobjective optimal design of Resonant Inductive Power Transfer (RIPT) devices. A thorough review of the literature has been performed in order to propose accurate analytical formulae for computing the lumped parameters of the system equivalent circuit. A particular attention is paid on the representation of the skin and proximity effects, and on the consideration of any relative position between the coils. The tool permits to observe design trends by comparing optimal individuals in the Pareto front, and is illustrated on an electric vehicle battery charging application. In that case, a design able to transfer 3 kW at 60 kHz, with 93.53 % efficiency through 25 cm air with a fixed radial space footprint of 25 cm, and capable to support a lateral misalignment of 10 cm, was obtained.

Index Terms—Design Optimization, Genetic Algorithms, Inductive Power Transfer

I. INTRODUCTION

Designing a Resonant Inductive Power Transfer (RIPT) device is not a trivial task, especially when high power (≥ 1 kW) needs to be transferred (*e.g.* for applications such as electric vehicles batteries charging). Indeed, it requires to achieve multiple and often conflicting objectives, such as to maximize the active power transmitted to the load and to maximize the efficiency of the transfer. The minimization of the working frequency is also a capital objective when high power is needed, since the technological constraints inherent to the power electronics supplies increase with the product of the power and the frequency. Moreover, the relations between the design parameters (*e.g.* the geometry of the coils) and the output quantities such as power and efficiency are not linear. Several deterministic design procedures are proposed in the literature. However, they often require the action of the designer in order to guide the optimization, and relate to an assisted trial-and-error methodology [1]. Evolutionary algorithms looking automatically for the optimal design, such as Genetic Algorithms (GAs), are investigated in [2] and [3]. Nevertheless, the first approach relies on mono-objective optimization and on approximate analytical formulae, and concerns low power/high frequency (up to several MHz) applications. Higher power systems are considered in the second work, but cumbersome numerical models are employed instead of analytical formulae. The design space related to the coil pattern is moreover very restricted.

In this work, the multiobjective Non-dominated Sorting Genetic Algorithm II (NSGA-II) [4] is employed for the design of WPT systems. Thanks to the use of the Pareto's theory, NSGA-II is able to determine the best tradeoffs between two

or more contradictory objectives. Thus, besides being able to design a specific setup, the proposed tool provides information about design trends by observing the optimal relation between the objective values of the individuals of the final population. The design procedure is thus more dynamic, making the strength of the proposed tool, much more interesting in comparison with deterministic tools. The WPT device is studied using a full analytical model based on the system equivalent circuit. Coils are modeled by lumped parameters computed with analytical formulae. Those formulae are derived from a thorough literature review and guarantee accuracy (by the inclusion of skin and proximity effects in the coil equivalent resistance) as well as more generality (by computing the magnetic coupling between coils in arbitrary relative position).

Section II describes the WPT system analytical model embedded in the GA procedure. A brief review of the analytical formulae used for the evaluation of the coils equivalent parameters is also presented. In section III, the optimization tool is described. For illustrational purpose, some results involving an electric vehicle application are presented and discussed in section IV. Finally, the section V draws the conclusions and perspectives of this paper.

II. MODELING OF THE WPT SYSTEM

The GA needs a model of the transfer device to link the design variables (geometry of the coils and characteristics of the source/load) to the objectives (output power and efficiency).

A. Equivalent circuit

In this work, the system is replaced by an equivalent circuit where the coils are modeled by lumped parameters (parasitic resistance R_i , self-inductance L_i , $i = 1$ for primary and $i = 2$ for secondary, and mutual inductance M_{12}). The source is replaced by its Thevenin equivalent circuit (V_S and R_S) and the load is represented by a resistance R_L . The compensation capacitances C_i ($i = 1, 2$) are computed using the resonant frequency f_0 value (shared by both primary and secondary) and the estimated self-inductance L_i of each coil ($C_i = L_i^{-1} (2\pi f_0)^{-2}$). The different positions of the compensation capacitances yield four possible topologies : series at both primary and secondary (SS), series at primary and parallel at secondary (SP), parallel at primary and series at secondary (PS) and parallel at both primary and secondary (PP). As an example, Fig. 1 shows the equivalent circuit for the SS topology. For each case, the currents and voltages in the corresponding circuit are solved by the use of the Kirchhoff's

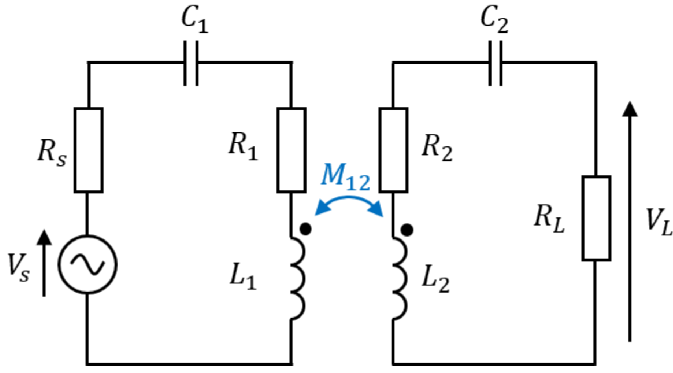


Fig. 1. Two-coil WPT system with SS topology equivalent circuit

circuit laws. Then, the input and output powers are deduced from these electrical quantities.

The use of analytical formulae for the computation of the coils lumped parameters is widely available and has been investigated in many studies. However, we pointed two important shortcomings that are recurrent in those works :

- 1) parasitic resistances are evaluated in DC conditions or even neglected. However, the skin and proximity effects appearing at the WPT operating frequencies can generate significant power losses for high power applications ;
- 2) the mutual inductance is computed with approximated formulae only applicable when the coils axes are aligned, while the coupling is a key factor in the transfer performances (in particular, regarding to the *frequency splitting* phenomenon [5]).

Thus, in this work, we propose to use more accurate and general formulae in order to model the transfer.

B. Formula of AC resistance

The resistance of a coil through which an alternative current flows increases considerably with the frequency due to skin and proximity effects. The AC resistance R_{AC} of a coil derives from the value of the DC resistance R_{DC} , estimated using the Pouillet's law, as follows :

$$R_{AC} = F_S \cdot (1 + G_P) \cdot R_{DC}. \quad (1)$$

The skin effect is rigorously modeled through the factor F_S given by [6] :

$$F_S = \frac{\alpha_0 \operatorname{ber}(\alpha_0) \operatorname{bei}'(\alpha_0) - \operatorname{bei}(\alpha_0) \operatorname{ber}'(\alpha_0)}{2 [\operatorname{ber}'(\alpha_0)]^2 + [\operatorname{bei}'(\alpha_0)]^2} \quad (2)$$

where $\alpha_0 = \sqrt{2} r_{wire} / \delta_{skin}$ (with δ_{skin} the skin depth and r_{wire} the wire radius), $\operatorname{ber}(x)$ and $\operatorname{bei}(x)$ are the Kelvin functions and $\operatorname{ber}'(x)$ and $\operatorname{bei}'(x)$ their derivative with respect to x .

The proximity effect is approximately estimated by the use of the proximity factor G_P [7]. It is tabulated for various values of the conductors spacing and numbers of turns in the case of antennas, assuming a high frequency. A comparison

with the resistance extracted from a 2D Finite Element tool [8] showed a relative error ranging from 10 % to 25 %. In fact, the analytical calculation of the exact resistance of a coil subject to proximity effect is still an open problem, which will be addressed in a future work.

C. Formulae of self and mutual inductances

Accurate analytical approaches to compute inductances only exist for single loops. In order to take profit from those approaches, the spiral coils of N turns involved in this work are approximated by a set of N concentric circular loops. The whole coil inductances are obtained by combining the individual loops parameters. The self-inductance L_l of a circular loop (radius r_l) made of round wire (radius r_{wire}) is evaluated in DC conditions since it is slightly affected by the frequency [9] :

$$L_l = \mu_0 r_l \left[\ln \left(\frac{8 r_l}{r_{wire}} \right) - 2 \right]. \quad (3)$$

As the self-inductance of a single loop, the mutual inductance between two loops is modeled without any influence of the frequency. Babic *et al.* have determined the analytical form of the mutual inductance between two loops arbitrarily positioned in space by the specification of each loop radius and the relative position of the loops [10]. The relative position is defined with a Cartesian description of the geometric problem. However, in this work, we will consider the coils either :

- 1) in the nominal position : aligned and separated by a distance d ;
- 2) in a deviated position : a lateral misalignment Δ is applied from the nominal position.

Thus, a description of the position using d and Δ is preferred here. The Babic's method has been adapted so that it becomes possible to express the mutual inductance M_{l-l} ($l-l$ standing for loop-to-loop) as a function of the radius of each filament and of the geometric parameters d and Δ :

$$M_{l-l,ij} = f(r_{l,i}, r_{l,j}, d, \Delta) \quad (4)$$

The self-inductance of the whole coil L_c incorporates the self-inductance of each single loop and the mutual inductance between each couple of loops constituting the coil :

$$L_c = \sum_{i=1}^N L_{l_i} + \sum_{i=1}^N \sum_{\substack{j=1 \\ j \neq i}}^N M_{l_i-l_j}. \quad (5)$$

The mutual inductance M_{c-c} ($c-c$ standing for coil-to-coil) between two coils (of N_1 turns and N_2 turns, respectively) is the sum of the mutual inductances between each loop of the first coil and each loop of the second coil :

$$M_{c-c} = \sum_{i=1}^{N_1} \sum_{j=1}^{N_2} M_{l_i-l_j}. \quad (6)$$

III. DESCRIPTION OF THE OPTIMIZATION TOOL

In this section, the optimization mechanism applied by NSGA-II is briefly described. The different quantities eligible as decision (or optimization) variables, constraints or objectives are quickly reviewed in order to enhance the possibilities offered by the proposed tool.

A. General principle of NSGA-II

NSGA-II has already been applied to solve many different problems in the field of electrical engineering. Indeed, it shows very good performances for global search of optimal solutions even for nonlinear problems involving both real and discrete parameters. The main principle is the following. A population where a given setup is represented by an individual whose genome is composed by the optimization variables relative to this setup is first established. Then, the evolution mechanism of natural selection is used to improve the adaptation of the individuals (by crossings and mutations) to the problem. The adaptation is evaluated through the individuals fitness to the objectives. The eventual constraint violations penalize the fitness associated with the violating individual leading to its removing in the selection step. The fulfilment of multiple and contradictory objectives is handled by the application of the Pareto's domination theory during the selection step. It guarantees that the final population contains the individuals ensuring the best compromise between the selected objectives. Finally, we have to precise that the diversity of the individual is guaranteed thanks to the computation of a distance in the objectives space and fostering the subsistence of isolated individuals.

B. Quantities eligible as decision variables

The quantities eligible as decision variables are the input parameters of the model of the transfer described in the previous section. Those parameters includes electrical quantities relative to the equivalent circuit : the source voltage, the source internal resistance, the supply frequency, the resonant frequency (conditioning the compensation capacitance value), the load resistance and the circuit topology. Some geometric parameters associated with the coils are also eligible : the inner radius, the wire radius, the number of turn(s) and the turns spacing of each coil, but also the distance and the lateral misalignment between the coils.

C. Quantities eligible as objective or constraint

The entire set of input parameters detailed previously is eligible as an objective or a constraint. Unlike decision variables, objectives and constraints can be quantities resulting from a process on the input variables. Most of the processes provided by the tool are related to electrical quantities : currents and voltages in the entire circuit and then, input and output (active and reactive) powers of the device and efficiencies. Geometric quantities can also be used in order to compute a space footprint associated with a given device.

IV. ILLUSTRATION ON AN ELECTRIC VEHICLE CHARGING APPLICATION

In this last section, the proposed tool is applied to the design of a WPT device for the charging of an electric vehicle battery. As mentioned before, this tool has the advantage to allow the extraction of design trends by studying the Pareto front (representation of the individuals in the objectives space) resulting from an execution of the GA. Different executions of the GA are considered in order to observe some of these design trends. In the last case, a particular individual is picked in the final population in order to show the tool's ability to also design a particular optimal setup.

A. Optimization environment

The general optimization environment used to extract the presented results is described here.

1) *Objectives:* The objectives change depending on the aim of each execution of the GA, *i.e.* the trend linking the optimal individuals the user want to observe.

2) *Decision variables:* In our example, the coils are considered identical. Their inner radius R_{in} is a real decision variable. The gap between two subsequent turns δ_{turn} is a discrete decision variable coded by 2 bits since the proximity factor G_p is tabulated only for discrete values of the spacing between turns. The number of turns N is a discrete decision variable coded by 4 bits so that the maximum number of turns is 15. Moreover, the GA is also free to choose the right compensation topology of the setup. Thus, this parameter is a discrete decision variable coded by 2 bits (enough to represent the 4 possible topologies).

3) *Constraints:* As a reference, a wire connected EV charger supplies typically 3.3 kW. In order to observe the evolution of the transmissible power depending on the other parameters, the power of the designed wireless charger is allowed to vary from 3 kW to 4 kW. The transfer frequency is limited to 100 kHz in order to limit the technological constraints on the power electronics source converter. The radial space footprint of the coils is limited to 25 cm. The transfer distance d is fixed to 25 cm (corresponding to the average height of a car's underseal). The source (considered as ideal by canceling its internal resistance) supplies 100 V. The load is a resistance of 3 Ω . The section of the wire is fixed to 10 mm² since it has been observed that the GA will logically foster the maximum section allowed when it is left as a decision variable. The self-resonant frequency f_0 shared by both the primary and secondary is set equal to the supply frequency f since preliminary tests showed that the optimal solutions always tend to equal f and f_0 . The global design work considers logically the system in its nominal position, *i.e.* when the coils are aligned. The lateral misalignment of the coils is thus set to 0 except in the last execution which optimizes the device robustness to a misalignment.

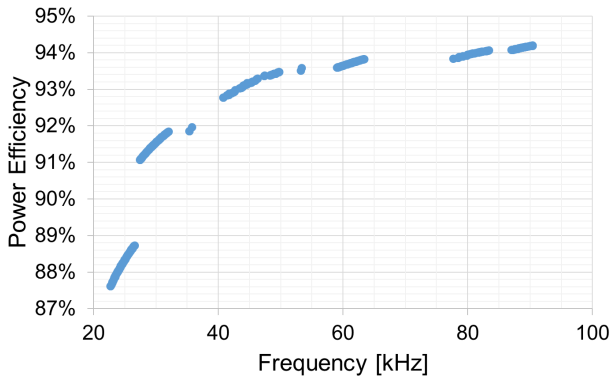


Fig. 2. Pareto front showing the optimal relation between frequency and efficiency in the nominal position

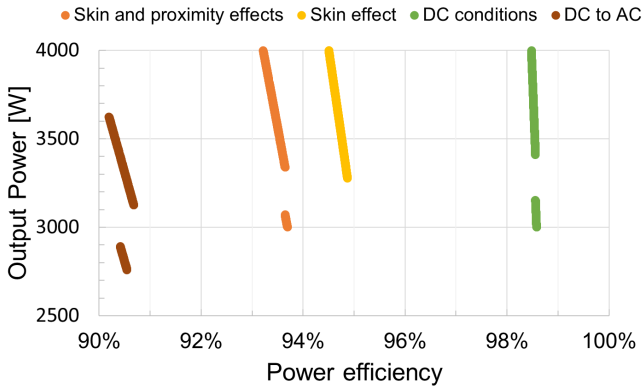


Fig. 3. Impact of the skin and proximity effects on the performances of optimal individuals

B. First execution : relation between frequency and efficiency

As mentioned above, a lower frequency involves lower technological constraints on the power electronics devices. On the other hand, the power efficiency increases with the working frequency. Thus, we can observe on Fig. 2 the Pareto front showing the best tradeoffs between the two following objectives : to maximize the power efficiency and to minimize the frequency. Interestingly, the power efficiency of the optimal individuals seems to saturate at a maximum value (the best affordable regarding the constraints) as the frequency increases. The designer can take advantage of this observation to adopt a frequency of 60 kHz, corresponding to an optimal efficiency of 93.5 %.

C. Second execution : impact of the skin and proximity effects

The tool is employed here to demonstrate the importance of the inclusion of AC effects on the evaluation of the system performances. A comparison of three different GA executions is proposed here. In every case, the objectives are to maximize the power efficiency and the output power but three different models of the WPT device are used: one with the inclusion of full AC (skin and proximity) effects, one with only skin effect and one in DC conditions. Frequency is fixed to 60 kHz according to the previous observation. The resulting Pareto

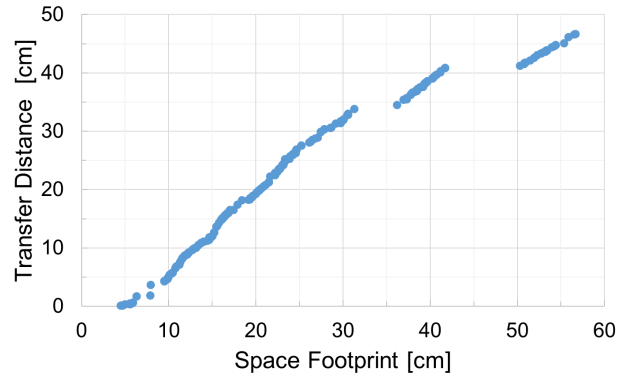


Fig. 4. Pareto front showing the optimal relation between transfer distance and space footprint in the nominal position

fronts (see Fig. 3) show clearly the impact of the AC effects on the optimal individuals with a maximal efficiency around 93.5 %, 94.5 % and 98.5 %, respectively. When the full AC model is applied a posteriori on the optimal individuals obtained in DC conditions, the efficiency decreases by 8.5 % to reach 90 % (see the DC to AC curve on Fig. 3). It is therefore imperative to embed the skin and proximity effects directly in the optimization tool, since the decision mechanism is able to provide individuals with better performances in that case (93.5 %, compared to 90 % in the a posteriori case).

D. Third execution : relation between transfer distance and space footprint

In some applications, it could be interesting to minimize the radial space footprint of the coils without neglecting the transfer distance. The two objectives are to maximize the transfer distance and to minimize the space footprint (left free to vary as decision variables in this case). The working frequency is fixed at 60 kHz and an additional constraint ensures that the efficiency is higher than 93 %. Results are presented on Fig. 4. We can observe that the transfer distance is almost equal to the radial space footprint for all the optimal individuals as expected in the domain of mid-range power transfer.

E. Fourth execution : robustness to a lateral misalignment

All the precedent executions of the GA suppose an ideal alignment of the coils. In a practical case, it seems difficult to align exactly the vehicle receiver with the floor transmitter. Maximizing the device robustness to a misalignment is therefore capital. Here, the two objectives are to maximize the lateral misalignment between the coils and to minimize the subsequent drop of efficiency (compared to the efficiency in nominal position). As in the last execution, frequency is fixed at 60 kHz and efficiency remains greater than 93 % in the nominal position. The Pareto front on Fig. 5 shows that the efficiency is decreasing quicker as the misalignment increases. Some individuals are able to transfer enough power with a 10 cm misalignment, with a drop of efficiency of 1 % only. The particular individual (whose parameters are highlighted

in the red box on Fig. 5) corresponding to that point can be picked to build a concrete device. In summary, it affords a 3 kW transfer through 25 cm air at 60 kHz, with a 93.53 % efficiency in nominal position, and supporting a 10 cm lateral misalignment with only a drop of 1 % on the efficiency.

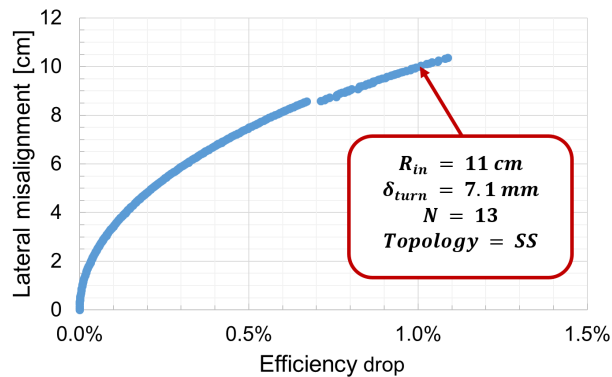


Fig. 5. Pareto front showing the optimal relation between lateral misalignment and the corresponding efficiency drop (compared to efficiency with a zero misalignment).

V. CONCLUSIONS AND PERSPECTIVES

In this paper, a multiobjective optimization tool is proposed for the design of two-coil WPT devices design. The system is represented by a full analytical model in order to avoid time- and resource-consuming numerical simulations. A literature review has been done to guarantee more generality and more accuracy compared to existing approaches. NSGA-II is employed so that the user can obtain dynamic design information, thanks to the Pareto's theory. The tool has been tested on an electric vehicle battery charging application. Interesting design trends have been observed. The importance of the inclusion of the AC effects on the coils resistance has been pointed out. The tool also showed its capacity to design a particular setup by picking an individual in the last test-case. Further work might extend the tool to four-coil WPT devices and also refine the modeling of the proximity effect.

ACKNOWLEDGMENT

The authors want to thank Dr Christophe Versèle for the development of NSGA-II in the MatLab environment.

REFERENCES

- [1] J. Sallan *et al.*, "Optimal Design of ICPT Systems Applied to Electric Vehicle Battery Charge, *IEEE Trans. Ind. Electron.*, vol. 56, no. 6, pp. 2140-2149, June 2009.
- [2] S. Lu *et al.*, "The Parameters Optimization of MCR-WPT System Based on the Improved Genetic Simulated Annealing Algorithm, *Hindawi Mathematical Problems in Engineering*, vol. 2015, 2015.
- [3] P. Ning *et al.*, "Genetic Algorithm based Coil System Optimization for Wireless Power Charging of Electric Vehicles, *IEEE Transp. Electr. Conf. Expo 2013*, pp. 1-5, June 2013
- [4] K. Deb *et al.*, "A Fast and Elitist Multiobjective Genetic Algorithmn : NSGA-II," *IEEE Trans. Evolutionary Computation*, vol. 6, no. 2, pp. 182-197, April 2002.
- [5] A. P. Sample *et al.*, "Analysis, Experimental Results, and Range Adaptation of Magnetically Coupled Resonators for Wireless Power Transfer, *IEEE Trans. Ind. Electron.*, vol. 58, no. 2, pp. 544-554, February 2011.
- [6] M. K. Kazimierczuk, *High-Frequency Magnetic Components*, J. Wiley & Sons, 2009.
- [7] G. S. Smith, *The proximity effect in systems of parallel conductors*, . J. Appl. Phys., May 1972.
- [8] A. Desmoort *et al.*, "A virtual laboratory for the modeling of Wireless Power Transfer systems , *Internat. Conf. on Electromagn. in Advanced Applications 2015* , pp. 1353 - 1356, September 2015
- [9] C. M. Zierhofer *et al.*, "Geometric approach for coupling enhancement of magnetically coupled coils," *IEEE Trans. Biomedical Engineering*, vol. 43, no. 7, pp. 708-714, July 1996.
- [10] S. Babic *et al.*, "Mutual Inductance Calculation Between Circular Filaments Arbitrarily Positioned in Space: Alternative to Grover's Formula," *IEEE Trans. Magnetics*, vol. 46, no. 9, pp. 3501-3600, April 2010.